Metrol. Meas. Syst., Vol. 29 (2022), No. 1
DOI: 10.24425/mms.2022.138543

METROLOGY AND MEASUREMENT SYSTEMS
Index 330930, ISSN 0860-8229
www.metrology.wat.edu.pl

PERIOD VERIFICATION DEVICE FOR VENTILATION RATE STANDARD RODS BASED ON A DIGITAL THERMAL FLOWMETER

Jiacheng Hu[1)], Ying Sha[1)], Jinhui Cai[1)], Ying Liu[2)], Suijun Liu[3)]

1) *China Jiliang University, NO.258 XueYuan Street, Hangzhou, China* (✉ *hujiacheng@cjlu.edu.cn*, +86 159 8819 9329, *P20020854066@cjlu.edu.cn*, *caijinhui@cjlu.edu.cn*)
2) *Technology Center of Henan China Tobacco Industry Co., Ltd., NO. 16 South YuLin Street, Zhengzhou, China* (*543112146@qq.com*)
3) *Nanyang Cigarette Factory of Henan China Tobacco Industry Co., Ltd., NO. 4 East XinHua Street, Nanyang, China* (*nyliusj@qq.com*)

Abstract

Ventilation rate is a physical index that is strictly controlled during cigarette manufacturing because an abnormal ventilation rate can affect the release of mainstream smoke, tar, and other components harmful to human health. Therefore, the standard rod is used for measuring the ventilation rate, which necessitates accurate and effective periodic inspections. In this study, we designed and built a set of special tobacco ventilation rate standard rods to assess the standard device during its verification period and used a digital thermal flowmeter as the flow standard. We determined the micro-pressure adjustment interval through fluid simulation, and conducted an experimental verification based on the simulation results. At the adjustment point where the differential pressure value was 0 Pa, the period verification device was tested under standard values of 27.38%, 58.83%, and 71.95%. The results show that the measurement errors of the device are -0.42%, 0.55%, and -0.13% respectively, which all meet the verification regulation requirements and indicate that the device is applicable in practical situations.

Keywords: ventilation rate standard rod, period verification, numerical simulation, digital thermal flowmeter, micro-pressure difference adjustment

1. Introduction

Ventilation rate is one of the primary determinants of pollutant levels from cigarettes, such as carbon monoxide (CO), nicotine, and tar. The ventilation rate considerably affects the emission of smoke, which is harmful to human health. Hence, this parameter is strictly controlled during cigarette processing and manufacturing [1-3]. At present, most cigarette-processing enterprises rely on comprehensive test benches to measure the ventilation rate of finished cigarettes. The most commonly used are the SODIMAT D49 comprehensive test bench (SODIM, France) and the DT-5 comprehensive test bench (Borgwaldt, Germany).

The measurement accuracy of the comprehensive test bench ventilation rate testing unit mainly depends on the ventilation rate standard rod used to calibrate it. Therefore, the measurement accuracy of the standard rod is particularly important. According to "China JJG (Tobacco) 17-2002: Regulations for the verification of tobacco ventilation rate standard rods" [4], the verification period of the ventilation rate standard rods is one year. However, in the actual production and consumption timeframe, ventilation rate standard rods suffer from blockage, ageing, pollution, and damage to the vent of the bar, which significantly reduces the accuracy of this component. Therefore, it is necessary to inspect ventilation rate standard rods periodically to prevent the production of substandard cigarettes and prevent smokers from having their health negatively affected due to excessive smoke inhalation.

Article history: received May 31, 2021; revised August 31, 2021; accepted September 10, 2021; available online October 17, 2021.

Conventionally, ventilation rate is detected using a soap film flowmeter or a piston flowmeter as the flow measurement standard. Using a soap film flowmeter as the standard measurement device offers several advantages, such as lower pressure drops, which ensures high measurement accuracy due to the glass composition of the soap film tube. However, the addition of soap liquid causes changes in the humidity along the gas path, which affects the viscous resistance of the pipe wall, creates a difference between the gas flowing through the soap film flowmeter and the measured gas, and affects the overall measurement. In addition, when measuring a small flow of gas, issues related to diffusion occur, which further affect the measurement results [5]. Furthermore, visual observation of the soap film's swimming position and timing using stopwatches during the measurement process invariably result in errors. Moreover, such manual methods are time-consuming, inefficient, and labour-intensive.

Similarly, when using a piston flowmeter as the standard measurement device, the reciprocating movement of the piston causes the gas in the tube to exhibit oscillations at different frequencies [6]. The repeated friction between the piston and the tube wall causes the temperature of the gas in the tube to change, resulting in a change in the gas viscosity; this affects the gap thickness and leakage flow [7-8] and leads to inaccurate measurements.

To address the limitations of the aforementioned methods, this paper proposes a novel micro-pressure adjustment scheme based on digital thermal flowmeters. In this work, the SIERRA 100 model was used. The measurement principle of the SIERRA 100 mass flowmeter is that gas molecules contact the heated sensor to complete heat conduction, making the sensor temperature change, and different gas molecules have various heat conduction capabilities. Therefore, the sensor temperature change can be directly measured. The amount of gas molecules flowing through is measured to obtain the mass flow rate of the gas, rather than the volume flow rate. Hence, the influence of temperature on the measurement process is avoided, and temperature compensation is not required. The response time of one measurement of the digital thermal flowmeter is less than 100 ms, and the response time of piston and soap film flowmeters is generally approximately 30 s. Thus, the choice of a digital thermal flowmeter can meet the requirements of this study. Based on the digital thermal flowmeter, a differential pressure gauge and a needle valve are introduced to adjust the micro differential pressure, and the effectiveness of the scheme described in this article is verified through simulation and experiments. We believe that the proposed method will contribute to more accurate ventilation rate measurements and transmission values during cigarette processing and manufacturing.

2. Ventilation rate measurement principle based on a digital thermal flowmeter

2.1. Necessity of pressure difference compensation in ventilation rate measurement using a digital thermal flowmeter

In this study, a digital thermal flowmeter was used to replace the traditional soap film and piston flowmeters to avoid changing the gas composition in the gas path and prevent measurement errors.

However, when the airflow enters and exits the thermal flowmeter, the airflow cannot immediately adhere to the new pipe wall because of the inertia of the fluid. This results in the appearance of a series of tiny vortices that cause the fluid clusters to rub against each other and irreversibly transform a part of the mechanical energy. The internal energy causes the gas flow rate to decrease. The local loss of energy per unit weight of the fluid is defined as

$$h_{\varsigma} = \varsigma \frac{v^2}{2g}, \tag{1}$$

where ς is the local loss coefficient and v is the average flow velocity of the fluid in the pipe after the local loss.

Concurrently, the introduction of flowmeters also causes local pressure loss, as shown in (2).

$$\Delta p = \varsigma \frac{\rho v^2}{2}, \tag{2}$$

where Δp is the pressure difference before and after flowing through the flowmeter and ρ is the fluid density. Moreover, the Mach number is less than 1 as the highest gas velocity in the tube during the verification process is 7 m/s; this indicates that the gas is incompressible. Thus, ρ has a fixed value.

The local pressure loss changes the gas pressure drop model of the tobacco-specific ventilation rate standard rod, as shown in Fig. 1. In the figure, P1–P10 represent the pressure distributions in the 10 ventilation pipes inside the ventilation rate standard bar, P12 represents the pressure distribution at the side hole, and P11 and P13 represent the pressure distributions in the pipe that penetrates the side hole on both sides of the side hole.

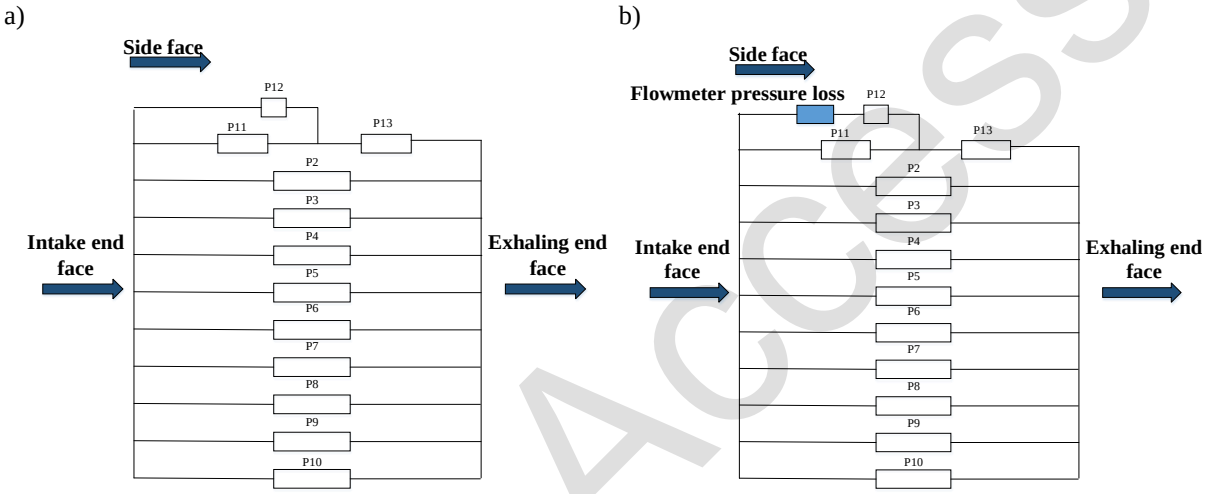

Fig. 1. Ventilation rate standard rod pressure drop model: a) no flowmeter introduced; b) flowmeter introduced.

In summary, a large pressure loss will be generated at the side hole, and the side hole airflow Q_1 (ml/s) will also be reduced when a digital thermal flowmeter is introduced into the system. In addition, the total airflow Q_2 (ml/s) generated by the constant flow hole will remain unchanged. Therefore, the measured value of the ventilation rate $V = \frac{Q_1}{Q_2} \times 100\%$ will be too small.

2.2. Measurement principle of digital thermal flowmeter

When the digital thermal flowmeter is energized, the two platinum resistance wire windings (*i.e.*, the two upstream and downstream coils) conduct a specific amount of heat H (constant) to the airflow. The temperatures of the two platinum resistance wire windings are equal but slightly higher than the actual gas temperature.

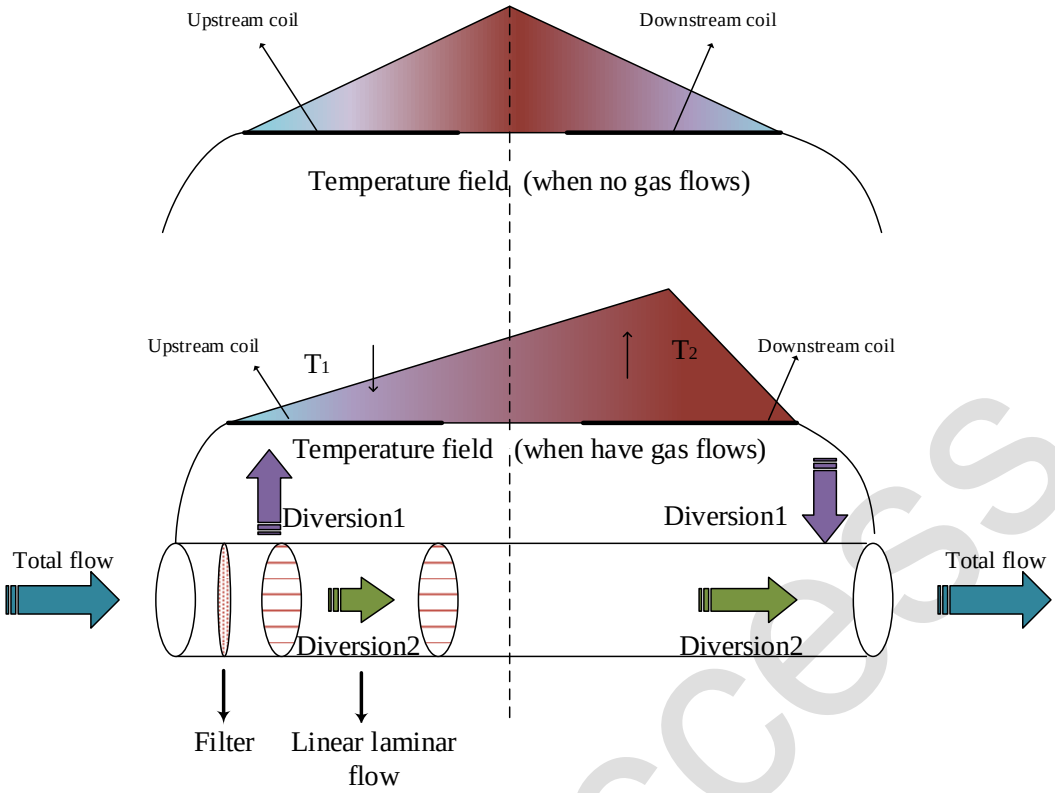

Fig. 2. Measuring principle of digital thermal flowmeter.

As shown in Fig. 2, when the measured gas does not flow through the pipeline, the temperature at the centre of the internal temperature field of the instrument is the highest, and the temperature gradually decreases from the middle to the sides. When the measured gas flows through the sensor from the left side, it absorbs the heat on the upstream coil and passes it to the downstream coil. Consequently, the temperature field distribution curve shifts to the right, resulting in a temperature difference ΔT $(\Delta T = T_2 - T_1)$. The total gas flow is directly proportional to ΔT. With regard to the resistance values of the two platinum resistance wires, when the phase difference is large, the resistance change can be converted into a voltage change through a bridge circuit. Then, the signal is transmitted to the processing circuit for filtering and amplification, conversion calculation, and other processing steps. Finally, the gas mass flow rate of diversion 1 can be obtained using the following equation.

$$\mathrm{m} = \frac{H}{C_p \times \Delta T}, \tag{3}$$

where H denotes the heat generated when the platinum resistance wire is energized; C_p represents the specific heat capacity at constant pressure; and ΔT denotes the temperature difference.

Owing to the uniform flow splitting effect of the laminar flowmeter, the gas mass ratio of diversions 1 and 2 is constant within the range of the digital thermal flowmeter; thus, the total gas mass flow can be obtained from the gas mass flow of diversion 1.

2.3. Ventilation rate measurement method based on micro-pressure difference adjustment using a digital flowmeter

A combined adjustment of the precision needle valve and differential pressure gauge was adopted in this study to compensate for the inherent pressure drop of the digital thermal

flowmeter [9, 10]. This addressed the problem described in Section 2.1, as shown in Fig. 3. The needle valve was adjusted to ensure that the pressure environment in the two air inlets would be the same, and the differential pressure sensor 2 (position 8 in Fig. 3) was used to monitor the pressure difference between the two gas paths.

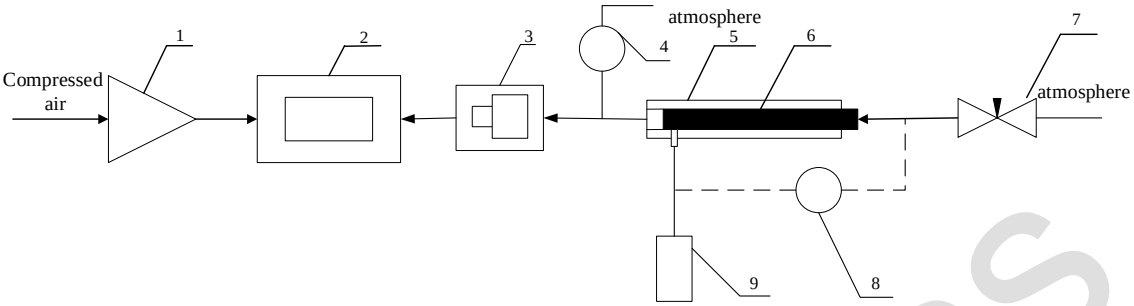

Fig. 3. Diagram of the differential pressure compensation principle for ventilation rate measurement based on a digital thermal flowmeter: 1. gas pressure regulator; 2. negative pressure generator; 3. tobacco special standard constant flow hole; 4. differential pressure sensor 1; 5. special fixture; 6. tobacco special ventilation rate standard rod; 7. needle valve; 8. differential pressure sensor 2; 9. digital thermal flow sensor.

The ventilation rate of the pressure difference compensation method in this study is defined in (4).

$$V_F = \frac{Q_M}{Q}\frac{P}{P - P_D} \times 100\%, \tag{4}$$

where Q_M is the side ventilation flow measured by the digital thermal flowmeter (ml/s), Q is the fixed total air flow (ml/s), P is the atmospheric pressure of the experimental environment (Pa), and P_D is the pressure measured by differential pressure sensor 1 (Pa).

3. Selection of the micro-pressure difference adjustment interval

Fluent, a fluid simulation software [11-13], was used to accurately locate the adjustment interval of the micro-pressure difference. According to a set ventilation rate of 27.38% and an error margin of ±1%, the pressure difference between the side inlet end face and the outlet end face changed several times. Thus, the pressure difference compensation process was simulated, and the simulation results are shown in Table 1.

Table 1. Changes in ventilation rate with different pressure differences.

Pressure compensation value(Pa)	-50	-40	-30	-20	-10	0	10	20	30
Ventilation rate (%)	28.37	28.20	28.11	27.90	27.71	27.38	26.90	26.52	26.37

The simulation results of the compensation process were fitted to the data, which yielded the fitting curve shown in Fig. 4.

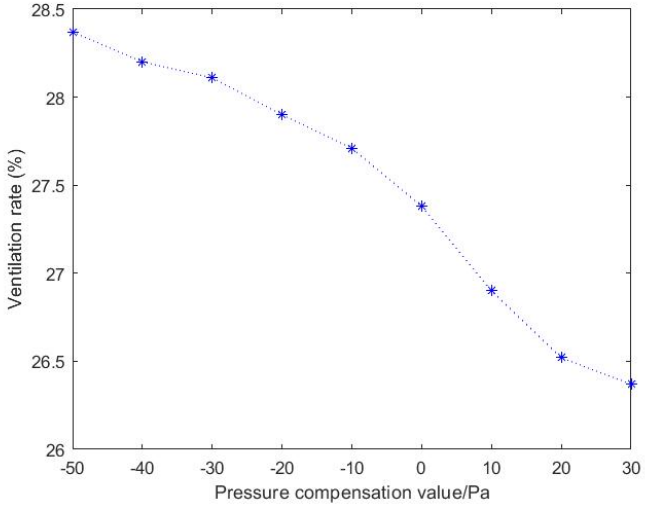

Fig. 4. Ventilation rate curve under different pressure differences.

Evidently, the smaller the pressure difference, the greater the ventilation rate. When the pressure difference between the two ends was within (-50~30) Pa, the ventilation rate fluctuated within the allowable range of ±1%.

The simulation results show that the opening of the needle valve needs to be adjusted to restrict the pressure difference gauge display value within (-50~30) Pa when the needle valve and differential pressure gauge are used to compensate for the pressure difference of the digital thermal flowmeter. At this time, the pressure at the side and end of the ventilation rate standard rod can be balanced to increase the accuracy of the ventilation rate measurement result.

4. Pressure regulation and flow compensation test experiment

After the construction of the experimental device and the completion of the experiment, ventilation rate standard rods verified by the China Tobacco Research Centre were used to validate the proposed scheme. The ventilation rate verification values were 27.38%, 58.83%, and 71.95%, which are used as standard values. The experimental environment must be stably maintained at a temperature of (22 ± 2) ºC, a relative humidity of (60 ± 5) %, and an atmospheric pressure of (96 ± 10) kPa. The experimental device is shown in Fig. 5.

a)

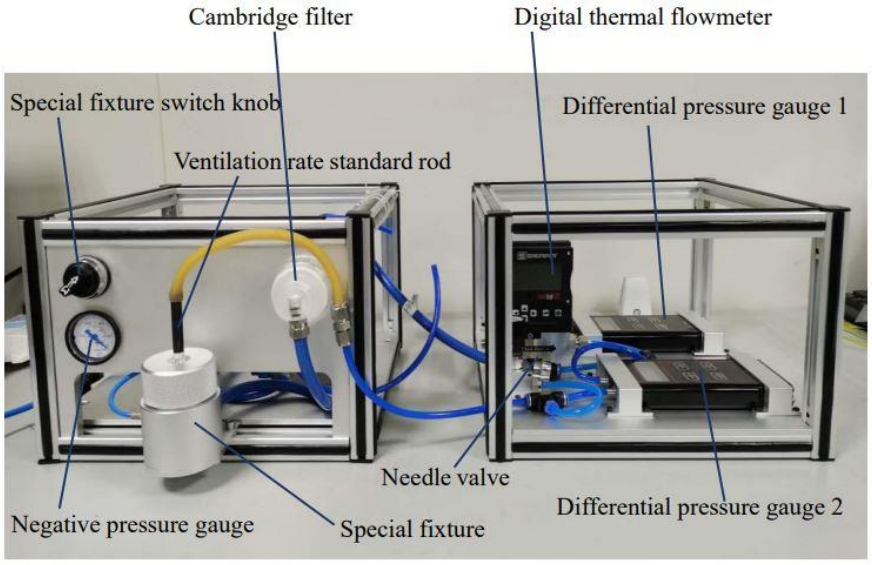

b) c)

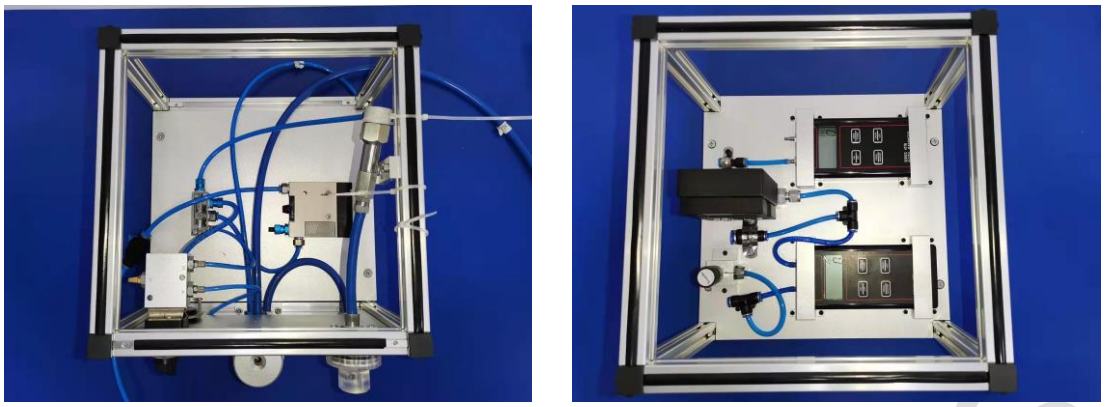

Fig. 5. Overall experimental installation set-up a) with the top views of the left b) and right boxes c).

4.1. Standard rod ventilation rate test experiment under uncompensated conditions

First, the three ventilation rate standard rods were tested without the addition of the pressure adjustment and flow compensation parts. The experimental data were substituted into (4) to calculate the ventilation rate, and the error value was compared with the verification value. Following, the specific experimental results are presented in detail.

For the standard rods with a ventilation rate of 27.38%, 58.83%, and 71.95%, the experimental conditions without the compensation adjustment device are listed in Tables 2–4, respectively. The respective average ventilation rates obtained were 17.05%, 27.43%, and 38.28%, with an error of 10.33%, 31.39%, and 33.67%, respectively. It is worth noting that the average ventilation rate of the rod with a ventilation rate of 71.95% was significantly smaller than the verification value.

Table 2. Measured parameters of the standard rod with a 27.38% ventilation rate without pressure adjustment and flow compensation.

Exp no.	Total flow (ml/s)	Side flow (ml/s)	P_D1 (Pa)	Average total flow (ml/s)	Average side flow (ml/s)	Ventilation rate (%)	Error (%)
1	17.280	2.922	-886	17.286	2.922	17.05	-10.33
2	17.290	2.923	-886				
3	17.290	2.921	-886				
4	17.290	2.922	-886				
5	17.280	2.921	-886				

Table 3. Measured parameters of the standard rod with a 58.83% ventilation rate without pressure adjustment and flow compensation.

Exp no.	Total flow (ml/s)	Side flow (ml/s)	P_D1 (Pa)	Average total flow (ml/s)	Average side flow (ml/s)	Ventilation rate (%)	Error (%)
1	17.280	4.710	-703	17.286	4.711	27.43	-31.39
2	17.290	4.711	-703				
3	17.290	4.712	-703				
4	17.290	4.711	-703				
5	17.280	4.710	-703				

Table 4. Measured parameters of the standard rod with a 71.95% ventilation rate without pressure adjustment and flow compensation.

Exp no.	Total flow (ml/s)	Side flow (ml/s)	P_D1 (Pa)	Average total flow (ml/s)	Average side flow (ml/s)	Ventilation rate (%)	Error (%)
1	17.280	6.544	-1160	17.286	6.544	38.28	-33.67
2	17.290	6.543	-1160				
3	17.290	6.544	-1160				
4	17.290	6.544	-1160				
5	17.280	6.543	-1160				

In summary, the ventilation measured values rate were not within the ±1% range required as per the verification regulations when the compensation devices were not added. Moreover, the errors for the three cases were relatively large. The results show the necessity of adding a compensation device to the proposed scheme.

4.2. Test on micro-pressure difference adjustment interval under compensated conditions

Without changing the aforementioned experimental environment, the pressure adjustment and flow compensation parts were added to the device, and the ventilation rate measurement experiment was conducted on the three standard rods investigated in this study. The needle valve was adjusted according to the simulation results presented in Section 2 so that the indicated value of the differential pressure gauge 2 is within ±50 Pa. The values measured by the digital thermal flowmeter (*i.e.*, side flow) and differential pressure sensor 1 (*i.e.*, the differential pressure between the inlet and outlet end faces of the ventilation rate standard rod) were recorded. The experimental data were substituted into (4) to calculate the ventilation rate, which was compared with the verification value to determine the error. Following, the specific experimental results are presented.

Tables 5–7 show the experimental results for the standard rods with a ventilation rate of 27.38%, 58.83%, and 71.95%, respectively, after the addition of the compensation device. The fitting curves in Figs. 6–8 represent the relationship between the pressure compensation values and the ventilation rate errors in Tables 5–7, respectively.

Table 5. Measured parameters of the standard rod with a 27.38% ventilation rate with pressure adjustment and flow compensation.

Exp no.	P_D2 (Pa)	Total flow (ml/s)	Side flow (ml/s)	P_D1 (Pa)	Ventilation rate(%)	Error(%)
1	-50	16.13	4.482	-1295	28.14	0.76
2	-40	16.13	4.446	-1281	27.91	0.53
3	-30	16.13	4.408	-1267	27.67	0.29
4	-23	16.13	4.380	-1260	27.49	0.11
5	-10	16.13	4.321	-1245	27.12	-0.26
6	0	16.13	4.267	-1228	26.78	-0.60
7	8	16.13	4.253	-1222	26.69	-0.69
8	15	16.13	4.232	-1214	26.55	-0.83
9	24	16.13	4.191	-1203	26.29	-1.09
10	30	16.13	4.168	-1195	26.14	-1.24

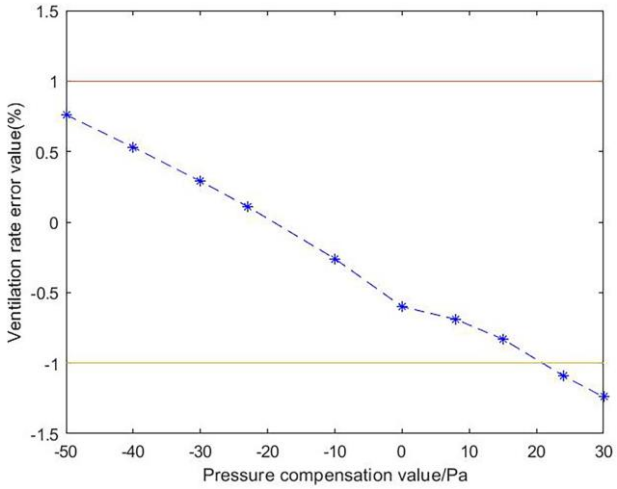

Fig. 6. Relationship between the experimental and verification values for the standard bar with a 27.38% ventilation rate.

Table 6. Measured parameters of the standard rod with a 58.83% ventilation rate with pressure adjustment and flow compensation.

Exp no.	P_D2 (Pa)	Total flow (ml/s)	Side flow (ml/s)	P_D1 (Pa)	Ventilation rate(%)	Error(%)
1	-21	16.08	9.633	-1556	60.83	2.00
2	-15	16.08	9.550	-1541	60.30	1.47
3	-8	16.08	9.495	-1534	59.95	1.11
4	0	16.08	9.445	-1526	59.63	0.80
5	7	16.08	9.401	-1512	59.34	0.51
6	15	16.08	9.273	-1493	58.52	-0.31
7	21	16.08	9.229	-1489	58.24	-0.59
8	30	16.08	9.135	-1475	57.64	-1.19
9	35	16.08	9.056	-1462	57.14	-1.69
10	44	16.08	8.994	-1449	56.74	-2.09

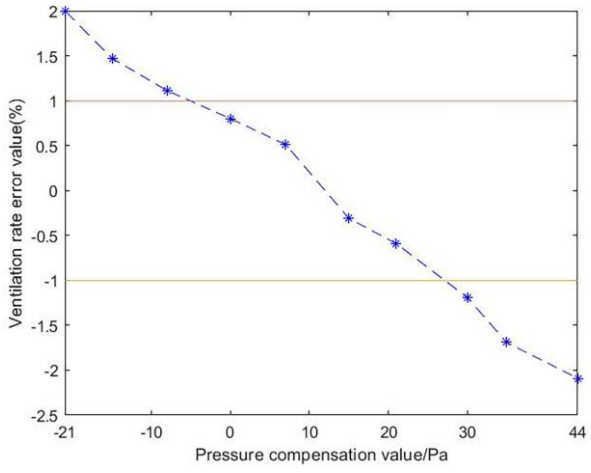

Fig. 7. Relationship between the experimental and verification values for the standard bar with a 58.83% ventilation rate.

Table 7. Measured parameters of the standard rod with a 71.95% ventilation rate with pressure adjustment and flow compensation.

Exp no.	P_D2 (Pa)	Total flow (ml/s)	Side flow (ml/s)	P_D1 (Pa)	Ventilation rate (%)	Error (%)
1	-27	16.7	11.96	-1930	73.00	1.05
2	-17	16.7	11.89	-1921	72.56	0.61
3	-10	16.7	11.82	-1914	72.13	0.18
4	-5	16.7	11.78	-1903	71.88	-0.07
5	0	16.7	11.74	-1900	71.63	-0.32
6	8	16.7	11.69	-1884	71.31	-0.64
7	14	16.7	11.62	-1881	70.89	-1.06
8	20	16.7	11.55	-1871	70.45	-1.50
9	30	16.7	11.47	-1860	69.96	-1.99
10	35	16.7	11.44	-1853	69.77	-2.18

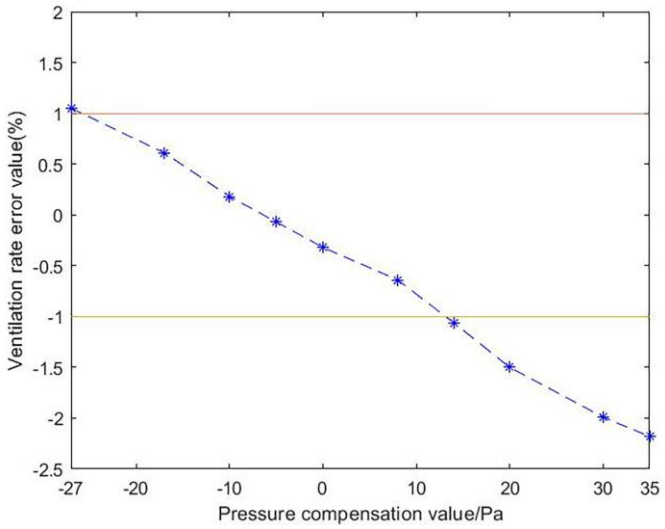

Fig. 8. Relationship between the experimental and verification values for the standard bar with a 71.95% ventilation rate.

In Figs. 6–8, the two solid lines represent the error limit of ±1% allowed under the standard ventilation rate values investigated in this study, and the dash-dotted lines represent the curves fitted to the error value of the ventilation rate. The experimental data show that the errors between the measured and standard values for standard rods with a ventilation rate of 27.38%, 58.83%, and 71.95% are within the limit corresponding to a pressure range of (-50~20) Pa, (-4~23) Pa, and (-26~12) Pa, respectively.

From the above experimental data, it can be seen that after adding the pressure adjustment and flow compensation parts, the best pressure compensation range of the three standard bars was measured: -50 to 20 Pa (27.38%), -4 to 23 Pa (58.83%), and -26 to 12 Pa (71.95%). The range of overlap between the three pressure compensation values was (-4~12) Pa. That is, when the needle valve is adjusted, the indication of the differential pressure gauge 2 is maintained within the interval of (-4~12) Pa, which has a good compensation effect for the ventilation rate measurement of the three ventilation rate standard bars investigated in this study. In addition, the pressure adjustment and flow compensation parts significantly improved the accuracy and repeatability of the measurement results. The experimental results thus confirm the validity of

the proposed compensation scheme for the inherent pressure drop of digital thermal flowmeters and the reliability of the developed device.

4.3. Repeatability test under compensated conditions

From Section 4.2, the optimal adjustment range for the pressure difference of the three standard rods is (-4~12) Pa. To facilitate the selection of compensation points during the actual verification, 0 Pa was selected as the optimal pressure compensation point of the device, and the ventilation rate experiment was repeated for the three standard rods. In addition, measurement experiments were conducted to verify the repeatability and accuracy of the proposed scheme. The test results on the standard rods with a ventilation rate of 27.38%, 58.83%, and 71.95% at an optimal pressure compensation point of 0 Pa are presented in Tables 8–10.

When the compensation pressure is 0 Pa, the ventilation rates corresponding to the standard values of 27.38%, 58.83%, and 71.95% are 26.96% (error of 0.42%), 59.37% (error of 0.55%), and 71.82% (error of 0.13%), respectively. The errors for the three standard rods are all within the limit of ±1% as per the verification regulations. Thus, the selection of compensation points is accurate and reliable.

Table 8. Measured parameters for the standard rod with a 27.38% ventilation rate at 0 Pa pressure compensation point

Exp no.	Pressure compensation value (Pa)	Total flow (ml/s)	Side flow (ml/s)	Average total flow (ml/s)	Average side flow (ml/s)	P_D1 (Pa)	Ventilation rate(%)	Error(%)
1	0	16.13	4.329	16.12	4.291	-1280	26.96	-0.42
2	0	16.13	4.267					
3	0	16.10	4.289					
4	0	16.13	4.285					
5	0	16.13	4.287					

Table 9. Measured parameters for standard rod with 58.83% ventilation rate at 0 Pa pressure compensation point.

Exp no.	Pressure compensation value (Pa)	Total flow (ml/s)	Side flow (ml/s)	Average total flow (ml/s)	Average side flow (ml/s)	P_D1 (Pa)	Ventilation rate(%)	Error(%)
1	0	16.08	9.445	16.13	9.442	-1447	59.37	0.55
2	0	16.12	9.434					
3	0	16.20	9.450					
4	0	16.12	9.443					
5	0	16.13	9.440					

Table 10. Measured parameters for standard rod with 71.95% ventilation rate at 0 Pa pressure compensation point.

Exp no.	Pressure compensation value (Pa)	Total flow (ml/s)	Side flow (ml/s)	Average total flow (ml/s)	Average side flow (ml/s)	P_D1 (Pa)	Ventilation rate(%)	Error(%)
1	0	16.70	11.74	16.58	11.69	-1880	71.82	-0.13
2	0	16.70	11.79					
3	0	16.30	11.53					
4	0	16.50	11.62					
5	0	16.70	11.76					

5. Conclusions

In this paper, a ventilation rate standard rod period verification method based on micro-pressure difference adjustment is proposed and a corresponding set of standard devices to address the insufficiency of existing verification methods is introduced. A digital thermal flowmeter was used as the standard device, and a needle valve and digital differential pressure gauge were used to compensate for the inherent pressure drop of the digital thermal flowmeter. This effectively prevented the various errors introduced in the piston and soap film flowmeters that are conventionally used. Accordingly, the micro-pressure adjustment interval was determined to be -4 to 12 Pa, and a repeatable ventilation rate test experiment was conducted at 0 Pa based on the simulation results and the micro-pressure adjustment interval experiment. The experimental results showed three types of ventilation. The errors for the rate standard bars relative to the verification values were 0.42%, 0.55%, and 0.13%, which are all within the limit of ±1%. This indicates that the proposed standard device meets the requirements specified in the verification regulations and can serve as a reference for future studies on tar content reduction in cigarettes.

Despite its advantages, this study has some limitations. To overcome these limitations, we plan to carry out further research as follows:

(1) The degree of measurement automation needs to be improved. Presently, the ventilation flow and total air flow are measured separately by manually plugging and unplugging the pipeline. In a subsequent development, the free switching of the gas path in the measurement pipeline could be studied to establish a more streamlined measurement process.

(2) Continue to improve the ventilation rate measurement scheme principle. Currently, the total air flow and side flow of the ventilation rate standard rod cannot be measured simultaneously. Accordingly, the total air flow and side flow could be measured simultaneously to measure the ventilation rate faster.

6. References

[1] Pang, Y., et al. (2012). The effect of ventilation dilution on cigarette combustion temperature and the release of main harmful components in mainstream smoke. *Tobacco Science and Technology*, *11*, 29-32.

[2] Purkis, W., Mueller, C., Intorp, M., & Seidel H. (2010). The influence of cigarette designs and smoking regimes on vapour phase. *Beiträge zur Tabakforschung/Contributions to Tobacco Research*, *24*(1), 33-46. https://doi.org/10.2478/cttr-2013-0879

[3] Jamil, H. J., Albahri, M. R. A., Al-Noor, N. H., Al-Noor, T. H., Heydari, A. R., Rajan, A. K., Arnetz, J., Arnetz, B., & Tawfiq, L. N. M. (2020). *Journal of Physics: Conference Series*, *1664*(1), 012127. https://doi.org/10.1088/1742-6596/1664/1/012127

[4] JJG (Tobacco) 17-2002, Verification Regulations for Tobacco Ventilation Rate Standard Rods.

[5] Guo, J., & Heslop, M. (2004). Diffusion problems of soap-film flowmeter when measuring very low-rate gas flow. *Flow Measurement and Instrumentation*, *15*(5), 331-334. https://doi.org/10.1016/j.flowmeasinst.2004.06.002

[6] Kutin, J., Bobovnik, G., & Bajsić, I. (2013). Dynamic pressure corrections in a clearance-sealed piston prover for gas flow measurements. *Metrologia*, *50*(1), 66. https://doi.org/10.1088/0026-1394/50/1/66

[7] Bobovnik, G., & Kutin, J. (2019). Experimental identification and correction of the leakage flow effects in a clearance-sealed piston prover. *Metrologia*, *56*(1), 015013. https://doi.org/10.1088/1681-7575/aaf5b3

[8] Kutin, J., Bobovnik, G., & Bajsić, I. (2015). Heat exchange effects on the performance of a clearance-sealed piston prover for gas flow measurements. *Metrologia*, *52*(6), 857. https://doi.org/10.1088/0026-1394/52/6/857

[9] Yan, R., & Xu, Z. (2017). Research on humidity compensation scheme of PVTt method gas flow standard device. *China Metrology*, (06), 92-93, https://10.16569/j.cnki.cn11-3720/t.2017.06.030 (in Chinese)

[10] Colard, S., Trinkies, W., Cholet, G., Camm, B., Austin, M., & Gualandris, R., (2004). Compensation for the effects of ambient conditions on the calibration of multi-capillary pressure drop standards. *Beiträge zur Tabakforschung/Contributions to Tobacco Research*, *21*(3), 167-174. https://doi.org/10.2478/cttr-2013-0777

[11] Jiang, Z., Ding, X., Zhao, H., & Su, Z. (2012). Research on pressure drop transfer standard based on CFD. *Advanced Materials Research*, *1898*, 542-543. https://doi.org/10.4028/www.scientific.net/AMR.542-543.1105

[12] Cheng, J. (2015). *Numerical simulation of internal flow of several tobacco-specific standard devices* [Doctoral dissertation]. China Jiliang University.

[13] Kazemi, A., Van de Riet, K., & Curet, O. (2017). Hydrodynamics of mangrove-type root models: the effect of porosity, spacing ratio and flexibility. *Bioinspiration & Biomimetics*, *12*(5), 1-24. https://doi.org/10.1088/1748-3190/aa7ccf

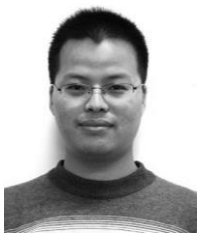

Jiacheng Hu received his Ph.D. degree from the University of Science and Technology of China in 2012. He is currently an Associate Professor in the Metrology and Testing Engineering Department in China Jiliang University. He has over 30 journal and conference publications and holds over 10 issued Chinese patents. His current research interests include new sensor detection technology and flow measurement technology.

Ying Sha received her B.Sc. degree in 2016 from China Jiliang University, where is she currently pursuing her master's degree. Her main research interests are precision instruments and machinery.

Jinhui Cai received his Ph.D. degree from the Zhejiang University in 2006. He is currently a Professor in the Metrology and Testing Engineering Department in China Jiliang University. His current research interests include metrology and industrial control.

Ying Liu received her B.Sc. degree in 2014 from Zhengzhou University of Light Industry. Now, she is working in Technology Center of Henan China Tobacco Industry Co., Ltd. Her main research interest is tobacco processing measurement technology.

Suijun Liu received his B.Sc. degree in 2018 from Nanyang Institute of Technology. Now, he is working in Nanyang Cigarette Factory of Henan China Tobacco Industry Co., Ltd. His main research interest is tobacco processing measurement technology.